Supporting Information: The Supernatant Phase in Polyelectrolyte Complex Coacervation: Cluster Formation, Binodal, and Nucleation

Pengfei Zhang*,† and Zhen-Gang Wang*,‡

†*State Key Laboratory for Modification of Chemical Fibers and Polymer Materials, Center for Advanced Low-Dimension Materials, College of Material Science and Engineering, Donghua University, Shanghai 201620, China*

‡*Division of Chemistry and Chemical Engineering, California Institute of Technology, Pasadena, CA 91125, United States*

E-mail: pfzhangphy@dhu.edu.cn; zgw@caltech.edu

S1. Chemical potential, osmotic pressure, binodal, and spinodal

From the bulk Helmholtz free density given by Eq. (5) of the main text, we calculate the chemical potential of polycation (or polyanion) per monomer as

$$\frac{\mu_p}{k_BT} = \frac{1+\ln\phi_p}{N_p} - \ln\left(1-2\phi_p-2\phi_s\right) - 1 + \frac{(l_B/\sigma)(2-\kappa\sigma)}{2(1+\kappa\sigma)} - \frac{4\pi\phi_p\left(l_B/\sigma\right)^2}{(1+\kappa\sigma)^2(\kappa\sigma)} \tag{S1}$$

and the chemical potential of small cation (or anion) as

$$\frac{\mu_s}{k_BT} = \ln \phi_s - \ln\left(1 - 2\phi_p - 2\phi_s\right) - \frac{4\pi\phi_p \left(l_B/\sigma\right)^2}{(1+\kappa\sigma)^2(\kappa\sigma)} - \frac{(\kappa\sigma)(l_B/\sigma)}{2(1+\kappa\sigma)}, \tag{S2}$$

respectively. The osmotic pressure is given by

$$\begin{aligned} \frac{\Pi v}{k_BT} &= \frac{2\phi_p}{N_p} - \ln(1 - 2\phi_p - 2\phi_s) - 2\phi_p - \frac{(l_B/\sigma)(\kappa\sigma)(\phi_p+\phi_s)}{1+\kappa\sigma} \\ &- \frac{8\pi\phi_p(\phi_p+\phi_s)\left(l_B/\sigma\right)^2}{(1+\kappa\sigma)^2(\kappa\sigma)} + \frac{1}{4\pi}\left[\ln(1+\kappa\sigma) - \kappa\sigma + \frac{(\kappa\sigma)^2}{2}\right]. \end{aligned} \tag{S3}$$

For the reservoir without polyions, the chemical potential of cation (anion) reduces to

$$\frac{\mu_s}{k_BT} = \ln \phi_{s,r} - \ln\left(1 - 2\phi_{s,r}\right) - \frac{(\kappa_r\sigma)(l_B/\sigma)}{2(1+\kappa_r\sigma)}, \tag{S4}$$

and the osmotic pressure in the resevior becomes

$$\frac{\Pi_r v}{k_BT} = -\ln(1 - 2\phi_{s,r}) - \frac{(\kappa_r\sigma)(l_B/\sigma)\phi_{s,r}}{1+\kappa_r\sigma} + \frac{1}{4\pi}\left[\ln(1+\kappa_r\sigma) - \kappa_r\sigma + \frac{(\kappa_r\sigma)^2}{2}\right], \tag{S5}$$

where $\phi_{s,r}$ is the cation (anion) concentration in the resevoir and $\kappa_r \equiv \sqrt{8\pi l_B \phi_{s,r}}$.

For two phases in coexistence, we denote the concentrations of polycation and cation in the supernatant phase by ϕ_p^{I} and ϕ_s^{I} respectively; likewise, the concentrations of polycation and cation in the coacervate phase are denoted by ϕ_p^{II} and ϕ_s^{II} respectively. Under the uniform mixing approximation, ϕ_p^{I}, ϕ_s^{I}, ϕ_p^{II}, and ϕ_s^{II} are determined by the phase equilibrium conditions, i.e, $\mu_p(\phi_p^{\mathrm{I}}, \phi_s^{\mathrm{I}}) = \mu_p(\phi_p^{\mathrm{II}}, \phi_s^{\mathrm{II}})$, $\mu_s(\phi_p^{\mathrm{I}}, \phi_s^{\mathrm{I}}) = \mu_s(\phi_p^{\mathrm{II}}, \phi_s^{\mathrm{II}})$, and $\Pi(\phi_p^{\mathrm{I}}, \phi_s^{\mathrm{I}}) = \Pi(\phi_p^{\mathrm{II}}, \phi_s^{\mathrm{II}})$. The procedures to construct the binodal can be found in Ref. S1 and will not be repeated here. In Figs. 4(a) and 7(b) of the main text, we present the binodals for symmetric mixtures without salt and in the presence of salt, respectively.

Under the uniform mixing approximation, the spinodal curve is determined by the vanishing of the determinant of the Hessen matrix for the bulk Helmholtz free energy (Eq. (5) of the main text), i.e.,

$$\left(\frac{\partial^2 f_b}{\partial \phi_p^2}\right)\left(\frac{\partial^2 f_b}{\partial \phi_s^2}\right) - \left(\frac{\partial^2 f_b}{\partial \phi_p \partial \phi_s}\right)^2 = 0, \tag{S6}$$

where

$$\frac{\partial^2 (f_b v/k_B T)}{\partial \phi_p^2} = \frac{2}{N\phi_p} + \frac{4}{1-2\phi_p-2\phi_s} - \frac{20\pi (l_B/\sigma)^2}{(1+\kappa\sigma)^2 \kappa\sigma} + \frac{32\pi^2 (l_B/\sigma)^3 (1+3\kappa\sigma)\phi_p}{(1+\kappa\sigma)^3 (\kappa\sigma)^3}, \tag{S7}$$

$$\frac{\partial^2 (f_b v/k_B T)}{\partial \phi_s^2} = \frac{2}{\phi_s} + \frac{4}{1-2\phi_p-2\phi_s} + \frac{32\pi^2 (l_B/\sigma)^3 (1+3\kappa\sigma)\phi_p}{(1+\kappa\sigma)^3 (\kappa\sigma)^3} - \frac{4\pi (l_B/\sigma)^2}{(1+\kappa\sigma)^2 \kappa\sigma}, \tag{S8}$$

and

$$\frac{\partial^2 (f_b v/k_B T)}{\partial \phi_p \partial \phi_s} = \frac{4}{1-2\phi_p-2\phi_s} - \frac{12\pi (l_B/\sigma)^2}{(1+\kappa\sigma)^2 \kappa\sigma} + \frac{32\pi^2 (l_B/\sigma)^3 (1+3\kappa\sigma)\phi_p}{(1+\kappa\sigma)^3 (\kappa\sigma)^3}. \tag{S9}$$

In Figs. 4(a) and 7(b) of the main text, we also present the spinodals for symmetric mixtures without salt and in the presence of salt, respectively.

S2. Properties of the polyion pair in the salt-free case

In Fig. S1, we show the polycation (polyanion) concentration $\phi_p(r)$ in a polyion pair (i.e., $m = 1$) at various l_B/σ, for solutions without small ions. We see that, with decreasing l_B/σ, polycation concentration inside the uniform core $\phi_{p,c} = \phi_p(r = 0)$ decreases and the interface becomes more diffusive. This feature is expected by noting that the electrostatic correlation that drives the formation of finite-sized clusters becomes weaker with decreasing l_B/σ.

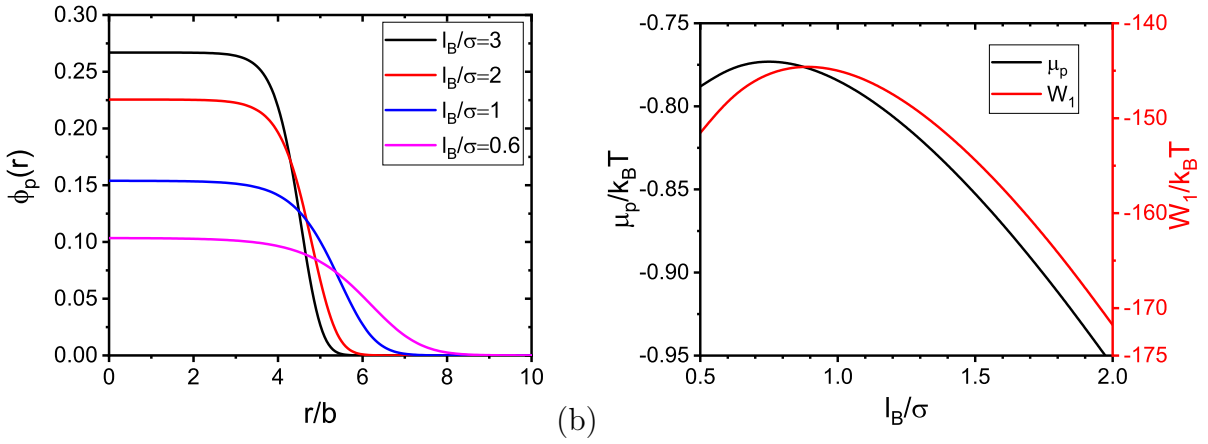

Figure S1: (a) Polycation (polyanion) concentration profile in a polyion pair (i.e., $m = 1$ cluster) in the absence of small ions. (b) Polycation chemical potential (per monomer) μ_p in the coacervate phase and free energy of a polyion pair W_1 as a function of l_B/σ. $N = 100$.

On the other hand, from Eq. (2) of the main text, we see the polycation concentration in an m-cluster ϕ_m can be determined once μ_p and W_m are known. For complex coacervation, at a given l_B/σ, μ_p can be determined by the polycation concentration in the coacervate phase $\phi_p^{\rm II}$ via Eq. (S1), and W_m is calculated numerically from the cluster structure using Eq. (10) from the main text. In Fig. S1(b), we show μ_p and W_1 as a function of l_B/σ, as an example. We see that both quantities exhibit a non-monotonic dependence on l_B/σ. With μ_p and W_1, we calculate the polycation concentration in one polyion pair ϕ_1, as shown by the blue dash curve in Fig. 3(b) of the main text.

S2. Properties of the polyion pair in the presence of small ions

In Fig. S2(a), we show the polycation (polyanion) concentration profile $\phi_p(r)$ of a polyion pair at various $\phi_{s,r}$, with $l_B/\sigma = 1.785$ fixed. With increasing $\phi_{s,r}$, the polycation concentration inside the uniform core of the cluster $\phi_{p,c}$ decreases and the interface becomes more diffusive. On the other hand, the cation (anion) concentration $\phi_s(r)$, as shown in Fig. S2(b), suggests that the cation concentration in the uniform core $\phi_{s,c}$ is lower than $\phi_{s,r}$ for all three

$\phi_{s,r}$. Moreover, we observe an enrichment of salt in the interfacial regime of the cluster, and the magnitude of this enrichment becomes weaker for larger $\phi_{s,r}$. This behavior is qualitatively consistent with the planer interface as examined in our previous work.[S2]

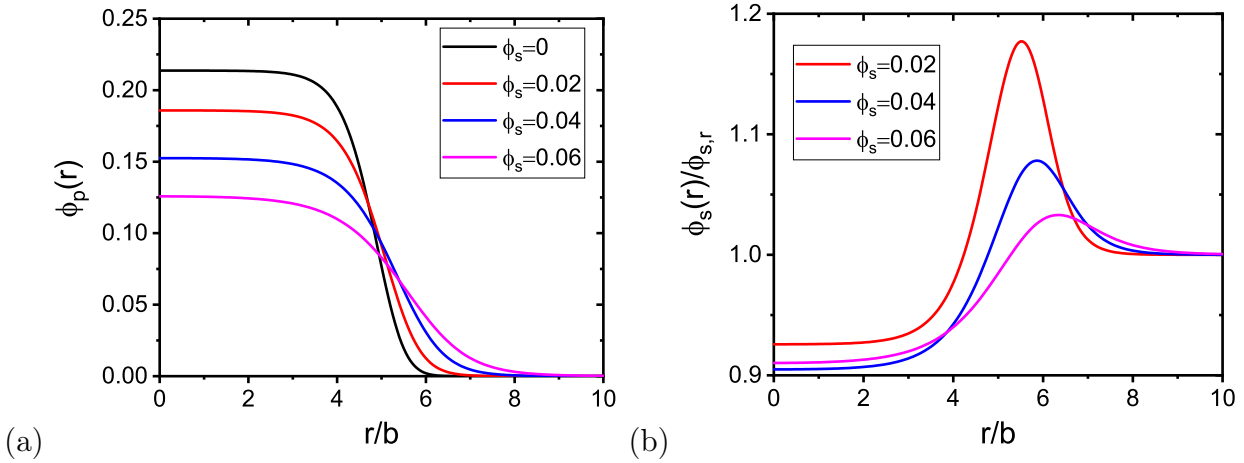

Figure S2: (a) Polycation (polyanion) concentration profiles, and (b) small cation (anion) concentration profiles for polyion pair (i.e., $m = 1$) at various $\phi_{s,r}$. $N = 100$ and $l_B/\sigma = 1.785$.

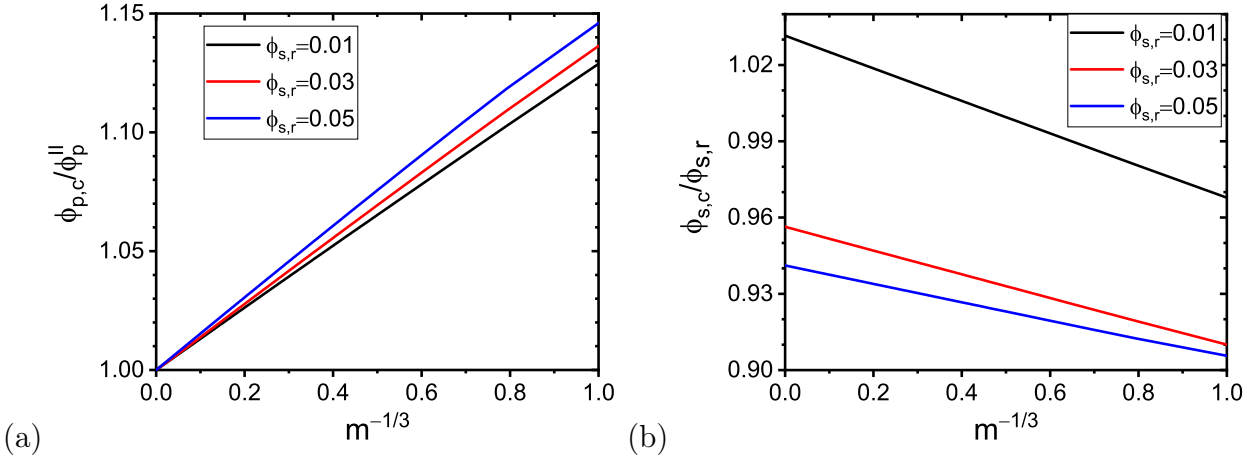

Figure S3: (a) Polycation (polyanion) concentration $\phi_{p,c}$ and (b) cation (anion) concentration $\phi_{s,c}$ in the uniform core of an m-cluster. $N = 100$ and $l_B/\sigma = 1.785$.

We also examine the m-dependence of $\phi_{p,c}$ and $\phi_{s,c}$ at different $\phi_{s,r}$ and show the results in Figs. S3(a) and (b) respectively. We see that $\phi_{p,c}$ decreases but $\phi_{s,c}$ increases with m. The leading order correction for both quantities is proportional to $m^{-1/3}$ at large m. These

features also result from the Laplace pressure effect as discussed in the main text. Moreover, we see that, in the limit of $m \to \infty$, $\phi_{s,c}/\phi_{s,r} > 1$ at $\phi_{s,r} = 0.01$. Since $\lim_{m\to\infty} \phi_{s,c} = \phi_s^{\mathrm{II}}$, this means that the salt concentration in the coacervate phase is higher than that in the reservoir; this partition behavior is opposite to the cases with $\phi_{s,r} = 0.03$ and 0.05. These salt partition behaviors are qualitatively consistent with our previous study.[S3]

References

(S1) Zhang, P.; Alsaifi, N. M.; Wu, J.; Wang, Z.-G. Polyelectrolyte Complex Coacervation: Effects of Concentration Asymmetry. *The Journal of Chemical Physics* **2018**, *149*, 163303, DOI: 10.1063/1.5028524.

(S2) Zhang, P.; Wang, Z.-G. Interfacial Structure and Tension of Polyelectrolyte Complex Coacervates. *Macromolecules* **2021**, *54*, 10994–11007, DOI: 10.1021/acs.macromol.1c01809.

(S3) Zhang, P.; Shen, K.; Alsaifi, N. M.; Wang, Z.-G. Salt Partitioning in Complex Coacervation of Symmetric Polyelectrolytes. *Macromolecules* **2018**, *51*, 5586–5593, DOI: 10.1021/acs.macromol.8b00726.